0273-2289/00/87/0037/$14.75

Continuous Production of Antibiotics in an Airlift Fermentor Utilizing a Transverse Magnetic Field

ZAKARIA AL-QODAH

Department of Chemical Engineering,
Amman College for Engineering Technology,
Al-Balqa Applied University, PO Box 340558, Marka, Amman, Jordan,
E-mail: zalqodah@hotmail.com

Received July 30, 1999; Revised November 24, 1999;
Accepted November 29, 1999

Abstract

In this study, a series of experiments was conducted to demonstrate the feasibility of continuous production of penicillin antibiotic using a three-phase magneto airlift fermentor with immobilized *Penicillium chrysogenum*. The fermentation processes were carried out in a 2.4-L external loop airlift utilizing a transverse magnetic field. It was found that the application of the magnetic field to a bed of ferromagnetic beads affects both the hydrodynamics of the reactor and the rate of the bioconversion process occurring inside it. One hundred hours after startup, the maximum penicillin concentration increased 48% as the magnetic field intensity increased from 0 to 35 mT, owing to the increased residence time of the substrate in the riser and the positive effect of the magnetic field on the effective fluid-solid interfacial area. In addition, the detached biomass concentration in the liquid phase was found to be only 5% of the immobilized biomass, owing to low shear levels and the absence of friction among the solid-phase particles.

Index Entries: Magnetic stabilization; magneto airlift reactors; magnetic field; penicillin production; *penicillium chrysogenum*.

Introduction

Whole-cell immobilization technology has generated considerable interest in the field of bioreactor design and operation. It has led to the design of new reactor configurations to accommodate the immobilized cell conformation that results in the formation of relatively large spherical

*Author to whom all correspondence and reprint requests should be addressed.

particles. Currently, fluidized beds and airlift bioreactors are being considered as promising types of reactors suitable for carrying out bioprocesses with immobilized whole cells. Compared to mechanically stirred vessels, these reactors are characterized by low shear stresses. For this reason, they seem to be quite attractive for use with shear-sensitive filamentous microorganisms such as *Penicillium chrysogenum*.

The airlift loop reactor is considered an alternative to the fluidized-bed reactor (FBR) in the search for a well-mixed and nonmechanically stirred immobilized cell reactor. An external (as opposed to an internal) loop reactor is the most widely used configuration because it has a more regular and well-defined flow pattern in addition to better degassing at the top of the reactor *(1)*.

Similar to the three-phase FBRs, airlift reactors suffer from the occurrence of large gas bubbles. This problem produces potentially disadvantageous outcomes, including a broad residence time distribution, imperfect contact of fluid phases, and a considerable backmixing of solids, which may reduce conversion via adsorption of reactants and products *(2,3)*.

For ideal operating conditions, in which adverse effects are minimized while maintaining the advantages, airlift loop reactors should have a plug flow in the gas phase and no backmixing in the solid phase. As the magnetic field suppresses the movements of the magnetic particles, an airlift reactor could be modified to the idea behavior by providing a solid phase of magnetic particles and applying the principle of magnetic stabilization. The application of the magnetic field to a bed of ferromagnetic particles induces magnetic cohesive forces among the particles, imposes anisotropy in their arrangement along the field lines, and suppresses bubble formation *(4–6)*.

Studies that give quantitative descriptions of the hydrodynamic behavior of magnetically stabilized beds (MSBs) have asserted that such operation provides an improved fluid-solid reactor. This reactor exhibits a combination of the best characteristics of both fluidized and packed beds *(7–12)*. Like fluidized beds, the stabilized bed has liquid-like properties, because its particles are easily transported. This facilitates good contact between the phases and the ability to combat bed clogging. In addition, MSBs usually operate at a bed pressure drop equal to the weight of the bed solids per cross-sectional bed area. This means that the pressure drop remains constant after bed expansion and is not affected by the particle size. Similar to what occurs in packed beds, bypassing of fluids, backmixing of solids, and particle washout are prevented in stabilized beds. Furthermore, compared to unstabilized beds, the particles do not suffer as much as with mechanical agitation, which leads to reduced catalyst attrition.

Many studies on MSBs have recently begun to exploit their properties in industrial applications such as chemical and biochemical processes, heat transfer, and several separation techniques *(13–17)*. Most of these studies have been limited to two-phase systems. Note that stabilization in transverse magnetic fields has rarely been investigated, unlike in axial magnetic fields *(18–20)*.

Limited information is available in the literature regarding the fundamental characteristics of three-phase systems in the presence of magnetic fields. Sada et al. *(21)* applied an axial magnetic field to a three-phase fluidized bed to keep magnetite-containing beads in the column over a wide range of fluid velocities. They found that the aggregation of the magnetic beads was not as pronounced as that in liquid-solid systems. Hu and Wu *(22)* studied the characteristics of three-phase fluidized beds in an axial magnetic field. Based on visual observations, they described the fluidization patterns and bed expansion under the influence of both the magnetic field intensity and the fluid velocities. Al-Qodah *(20)* studied the performance of a three-phase MSB bioreactor utilizing a transverse magnetic field. Some correlations regarding the effect of magnetic field intensity, fluid velocities on bed expansion, and minimum fluidization velocity were developed.

Recently, Ivanova et al. *(23)* studied the performance of an MSB reactor with immobilized yeast cells. They found that higher ethanol concentration and ethanol productivity were obtained. Subsequently, Colin et al. *(24)* applied an axial magnetic field to an immobilized enzyme reactor. They found that the overall mass-transfer rate was significantly improved.

In a more recent work, Thompson and Worden *(25)* studied phase holdup, liquid dispersion, and gas-to-liquid mass transfer in a three-phase fluidized bed utilizing an axial magnetic field. They found that, $K_L a$ either keeps constant or increases as the magnetic field increases, depending on the operating flow regime. In addition, they reported that the gas holdup decreased by as much as 20% of its value in the fluidized bed regime as the magnetic field intensity increased owing to bed contraction and the formation of preferred channels. Furthermore, a fourfold decrease in the axial dispersion coefficient was observed in the channel regime.

Al-Qodah *(26)* investigated the effect of the magnetic field on the hydrodynamics of three-phase gas-liquid-solid airlift reactors as an approach to improve their behavior. It was found that the application of the magnetic field to a three-phase airlift fermentor improves the mass-transfer characteristics, and affects liquid circulation velocity, bed expansion, coalescence of gas bubbles, and solid-phase distribution inside the reactor. It was concluded that a magneto airlift fermentor could be used as a suitable vessel for carrying out aerobic bioprocesses with immobilized cells such as filamentous fungi. For this reason, the aim of the present study was to demonstrate the applicability of magnetic stabilization for continuous bioprocessing in an airlift fermentor with immobilized cells. The production of the antibiotic penicillin G with immobilized *p. chrysogenum* was used as a model process.

Materials and Methods

Maintenance of Microorganism

All chemicals, unless stated otherwise, were purchased from Sigma (Poole, Dorset, UK). The culture *P. chrysogenum* was obtained as freeze-

dried ampoules from the Department of Applied Microbiology at Jordan University of Science and Technology. It was stored at 4°C as a silica gel stock. The procedure for microorganism maintenance was performed in a manner analogous to that used in Jones et al. *(27)*. Portions of the silica gel were dispersed onto the surface of sporulation agar in 500-mL Erlenmeyer flasks. The inoculated flasks were incubated at 26°C and 220 rpm in a gyratory water bath (New Brunswick, NJ) for 72 h. Spores were removed from the flasks with 5 mL of saline solution. The spore suspension obtained was used to inoculate the activated carbon magnetic beads or in submerged culture fermentation.

Preparation of Magnetic Support

Magnetic particles were prepared in the same manner as described previously *(28)*. Table 1 gives some of their characteristics. The magnetic particles consisted of a ferromagnetic core of magnetite (Fe_3O_4) covered with a stable layer of activated carbon in activated carbon 1 (AC1) and AC2 or zeolite in Z. Epoxy resin was used as an adhesive between the ferromagnetic core and the activated carbon or zeolite layers. Spherical magnetic beads with narrow size distribution were obtained. In addition, the magnetic beads were able to be sterilized because the activated carbon and zeolite layers were stable and could sustain the sterilization temperature.

Immobilization Method

The magnetic beads were first treated with 1% NaOH and 1% HCl and then washed with distilled water to neutral pH. After sterilization at 121°C in the presence of water (3 mL of water/1 g of beads) for 25 min, 270 g of the magnetic beads were cooled and mixed with 800 mL of spore suspension with a *P. chrysogenum* spore concentration of 1.1×10^8 spores/mL. This mixture was incubated at 26°C in a rotary shaker incubator at 120 rpm for 1.5 h. After the fixation process, the liquid was decanted, and the beads were washed with an abundant quantity of sterile water to remove the unfixed cells.

A growth medium was prepared in the same manner as described by Ariyo et al. *(29)*. This was added to the magnetic beads in the same proportions. The growth medium contained 20 g of sucrose, 10 g of lactose, 5 g of mycological peptone (Oxoid), 13 g of $(NH_4)_2SO_4$, 3 g of KH_2PO_4, 0.5 g of Na_2SO_4, 0.55 g of EDTA, 0.25 g of $MgSO_4 \cdot 7H_2O$, 0.05 g of $CaCl_2 \cdot 2H_2O$, 0.25 g of $Fe_2SO_4 \cdot 7H_2O$, 0.02 g of $MnSO_4 \cdot 4H_2O$, 0.2 g of $ZnSO_4 \cdot 7H_2O$, and 0.005 g of $CuSO_4 \cdot 5H_2O$ in 1000 mL of distilled water. The mixture of the growth medium and the loaded magnetic beads were incubated for 12 h at 26°C and 180 rpm to promote spore germination without loss of the spores from the magnetic beads. After 48 h of continuous growth, 200 mL of the medium was decanted, and the same volume of a fresh medium was added to compensate for the exhausted substrate. The magnetic beads were then washed with 2 vol of potassium phosphate buffer, pH 7.0. The washed magnetic beads were transferred to the reactor under sterile conditions.

Table 1
Characteristics of Magnetic Particles

Material used to cover magnetite	ρ_b (kg/m^3)	ρ_s (kg/m^3)	Shape factor	d_p (mm)	U_{mfo} (m/s)	M_s (mT)	Color (–)	Porosity (ε_o [–])	C_p (J/kg)
AC1	1750	3020	0.9	0.90	1.26	590	Black	0.42	362
AC2	1905	3230	0.9	1.05	1.48	590	Black	0.41	370
Z	2100	3500	0.8	1.20	1.83	590	Green	0.40	478

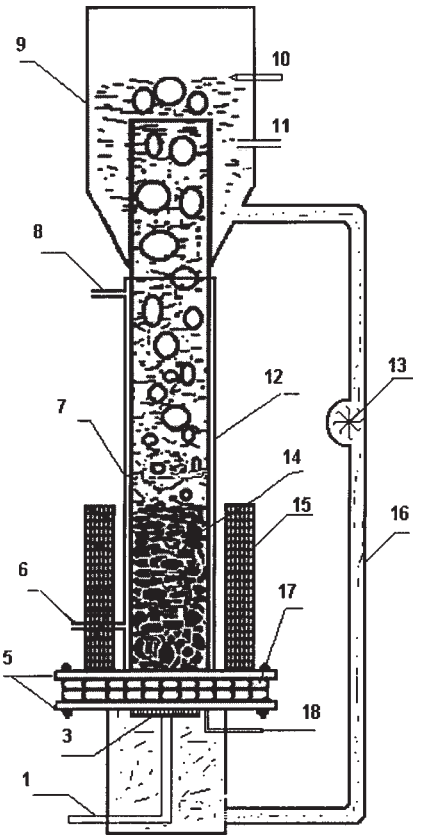

Fig. 1. Experimental apparatus. 1, Gas inlet; 2, circulating liquid inlet; 3, gas distributor; 4, supporting grid; 5, flanges; 6, water to the jacket; 7, jacket; 8, water from the jacket; 9, degassing section; 10, level controller electrode; 11, product outlet; 12, riser; 13, photo cell turbine; 14, magnetic particles; 15, magnetic system; 16, downcomer; 17, gaskets; 18, feed inlet.

Equipment for Continuous Fermentation

Figure 1 is a schematic diagram of the experimental setup. The external loop three-phase reactor was made of glass and consisted of a riser and downcomer tubes with inner diameters of 0.045 and 0.018 m, respectively. The heights of the riser and downcomer, H_r and H_d, were 0.7 and 0.72 m, respectively. The riser and the downcomer were 0.10 m apart. The column was surrounded by a water jacket, which was connected to a thermostat (Grant Instruments, Barrington, England) in order to maintain a constant fermentation temperature.

The degassing section consisted of a transparent cylinder with an inner diameter of 0.12 m and a height of 0.15 m and equipped with an air filter. This part was carefully designed to improve the degassing process in such a way that it would prevent circulation of the fine gas bubbles through the downcomer stream. This was accomplished by taking the downcomer flow

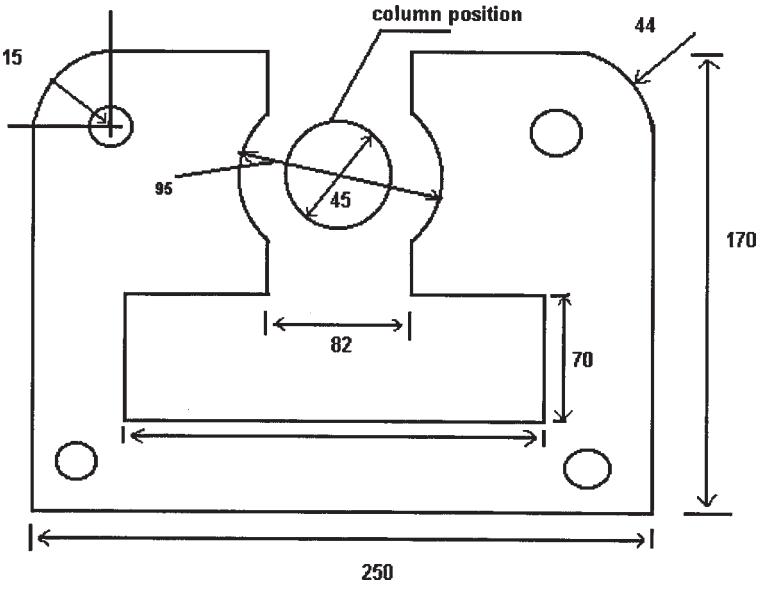

Fig. 2. Schematic diagram of a sheet of the magnetic system (dimensions in millimeters).

from a point 0.10 m below the top of the riser, as shown in Fig. 1. The total volume of the fermentor, including the riser, downcomer, degassing section, tubing, and joints, was 2.4 L. A perforated nonmagnetic stainless steel grid of 0.0003 m pore diameter was mounted on the base of the riser to support the magnetic beads and distribute the fluids. The bottom of the downcomer extended below the supporting grid and connected to the riser at a point 0.10 m below the gas distributor. This distance between the gas distributor and the bottom of the downcomer produced a head pressure sufficient to prevent the gas phase from entering the downcomer. Filtered air was injected through a +-shaped distributor with a 50-μm nominal pore size located 0.005 m below the supporting grid. This design gave an even distribution of gas bubbles over the entire cross-section of the riser.

The magnetic system was made of a cast steel core and 1500 copper coils made of a 0.9-mm copper wire. Glass wool was used as an insulator among the layers of coils. The core consisted of 180 painted 0.9-mm-thick cast steel sheets. The cast steel sheets were formed as shown in Fig. 2 in order to house the riser. The net height of the magnetic system was 0.2 m and its net weight was 40 kg. The direct current could be varied from 0 to 2.5 A, and the corresponding magnetic field intensity could be changed from 0 to 80 mT.

The production medium contained 10 g/L of lactose, 6.8 g/L of KH_2PO_4, 1.21 g/L of NH_4Cl, 1.0 g/L of phenylacetic acid (PAA), 3.95 g/L of K_2SO_4, and 0.25 g/L of $MgSO_4 \cdot 7H_2O$. The pH of the fermentation medium was adjusted to 6.8 with 2 *M* KOH before sterilization. This medium was fed to the riser at a point just below the supporting grid by a peristaltic pump (Gallen Kamp, Loughborough, UK) at a flow rate of 15 mL/h.

The dilution rate based on the volume of the magnetic beads (0.16 L) and that based on the whole reactor (2.4 L) were 0.094 and 6.25×10^{-3}/h, respectively. Antifoam 204 was used to minimize foaming in the bioreactor when necessary. Gas superficial velocity was maintained at 2.1 cm/s. This velocity was sufficient to induce liquid circulation between the riser and the downcomer. The magnetic field intensity was measured using a Hall sonde magnetometer (Leybolo-Heraeus, Berlin, Germany). During the course of fermentation, samples were collected periodically from the effluent stream; frozen; and later analyzed for lactose, penicillin G, PAA, and biomass.

Analytical Methods

Lactose in the samples was hydrolyzed by β-galactosidase from *Escherichia coli*. An enzyme kit based on glucose kinase and glucose-6-phosphate dehydrogenase (Boehringer Mannhein GmbH, Biochemica, Mannhein, Germany) was used to measure the released glucose. To determine the produced penicillin G and PAA in the broth, an off-line analysis for filtered samples was conducted by high-performance liquid chromatography (HPLC) (Hewlett Packard, Waldbronn, Germany). The high-performance liquid chromatograph was equipped with an S5C8 column (Hichrom, Reading, UK) eluted with a mobile phase containing 0.15 *M* potassium dihydrogen orthophosphate and 20% (v/v) acetonitrile. Detection of both materials was at 210 nm. Free biomass in the reactor medium was measured by filtering a 25 sample on 0.45-μm filter paper (MSI, Westboro, MA) by syringe filtration followed by drying the sample at 105°C until reaching a constant weight.

There are two modes of bed stabilization *(30)*: magnetizing first and magnetizing last. Experiments in the present study were conducted using the magnetizing first mode.

Results and Discussion

Description of Bed Behavior

Based on visual observations, we noticed that while maintaining a constant magnetic field intensity value (*B*), an increase in the gas velocity in the riser caused the bed structure to pass through the following regimes: the initial packed bed, the stable expanded bed, and the fluidized bed, respectively. These regimes correspond to the case in which the applied magnetic field intensity is more than 10 mT to induce strong cohesion forces among the magnetic particles. These forces influence the fluidization behavior of the bed because they tend to agglomerate the magnetic particles in the form of strings of relatively large volume.

Figure 3 gives the experimentally determined phase diagram for the magnetic particles used ($U_{mflo} = 0.0148$ m/s). It can be seen that for all values of the applied magnetic field intensity, the initial packed bed regime did not change until the gas velocity, U_g, exceeded a critical value called the

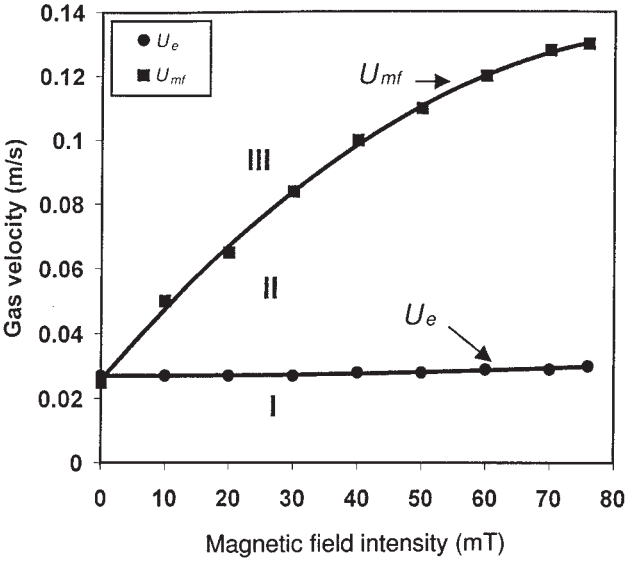

Fig. 3. Phase diagram for magneto airlift reactor charged with AC1 type magnetic particles (magnetizing first mode). I, packed bed; II, stabilized bed; III, fluidized bed.

minimum expansion velocity, U_e. Beyond this transitional velocity, which is represented by the lower curve in Fig. 3, the bed started to expand. Figure 3 shows that U_e was independent of the magnetic field intensity and remained constant and equal to 0.027 m/s. In the packed-bed regime, no motion or vibration of the magnetic particles was observed. Beyond the minimum expansion velocity, the bed began to expand stably but without particle movement or backmixing patterns. The bed continued to expand as the gas velocity increased, until the fluid velocity began to exceed a second transitional velocity called the minimum fluidization velocity, U_{mf}. The values of U_{mf} are represented by the upper curve in Fig. 3. The magnetized system operating at $U_e < U_g < U_{mf}$ was magnetically stabilized and resembled the "pseudopolymerized" and the stably fluidized-bed regimes described by Filippov *(7)* and Rosensweig *(4)*, respectively.

While passing through this stabilized regime, the bed continuously changes its structure by a process of piston-like slow and regular expansion to show minimum hydraulic resistance to the flowing fluids. Furthermore, the arrangement of the particle strings or chains along the field lines can be clearly observed in this regime. Similar to the situation in packed beds, the calm and stagnant strings suppress bubbles from coalescing. As a result, the gas phase in this regime consists of small, dispersed gas bubbles, and the bed appears bubble-free. In addition, only *in situ* vibrations of the strings, or chains of particles, are observed in the stabilized regime. The stabilized regime provides attractive conditions for bioprocesses with immobilized cells such as the fungus *P. chrysogenum*. These conditions include the absence of shear forces and the increased height of the bed, which result in longer residence time of the substrate and better aeration.

With a further increase in the gas velocity, radial cracks (slits) with relatively large gas bubbles emerge and grow in the stable bed until it breaks down at the minimum fluidization velocity, U_{mf}. Above this transitional velocity, the bed exists in the fluidized regime. In this regime, the fluidized system consists of strings (chains of particles). It is evident that in this regime, bubbles begin to coalesce to form relatively larger bubbles. For this reason, Rosensweig *(4)* called this regime the *bubbling regime*.

With a further increase in the gas velocity and if B values are <15 mT, the strings begin to separate into individual particles until the particulate fluidized bed is said to exist, and particles begin to be entrained to the degassing section. The fluidization behavior under these conditions resembles that of the conventional systems', which is characterized by intensive mixing among the phases and random motions of the fluidized particles.

While the transition between the initial packed- and stable-bed regimes, i.e., U_e curve, is seen to be independent on the magnetic field intensity, the onset of the fluidized-bed regime (and hence U_{mf}) can be increased to higher gas velocities by increasing the magnetic field intensity. For example, Fig. 3 shows that U_{mf} increases from 0.027 to 0.132 m/s as the magnetic field intensity increases from 0 to 80 mT. Furthermore, it is evident that the transition between each of these two regimes is sharp and reproducible.

The minimum fluidization velocity data shown in Fig. 3 are correlated to give Eq. 1:

$$U_{mf} = 0.6115 U_{mflo} B^{0.1588} \quad (1)$$

Values of the magnetic field intensity in this correlation range from 0 to 76 mT. The standard error of estimate (SEE) is 0.07.

In the present study only the effect of the magnetic field intensity on the gas velocity needed to fluidize the bed was considered, although the liquid phase is a fluidizing medium as well as the gaseous phase, and its velocity always increases as the gas velocity increases. This behavior of liquid velocity in airlift reactors is completely different from that in three-phase fluidized beds in which liquid velocity can be maintained constantly while varying the gas velocity. However, because the liquid velocity is a variable dependent on the gas velocity, it seems sufficient to consider the gas velocity as the fluidizing velocity.

Recently, Penchev and Hristov *(6)* termed the transitional velocity between the stable- and fluidized-bed regimes as the *minimum fluidization velocity*, U_{mf}, and that between the initial packed- and stable-bed regimes as the *minimum expansion velocity*, U_e. They based this on the fact that only beyond U_{mf} does the behavior of the bed particles resemble that at the onset of fluidization in unmagnetized beds; that is, the bed particles are able to change their places in the bed. In the present study, U_{mf} is defined as the transitional velocity between the stable- and the fluidized-bed regimes. Beyond this velocity, the stable bed is destroyed.

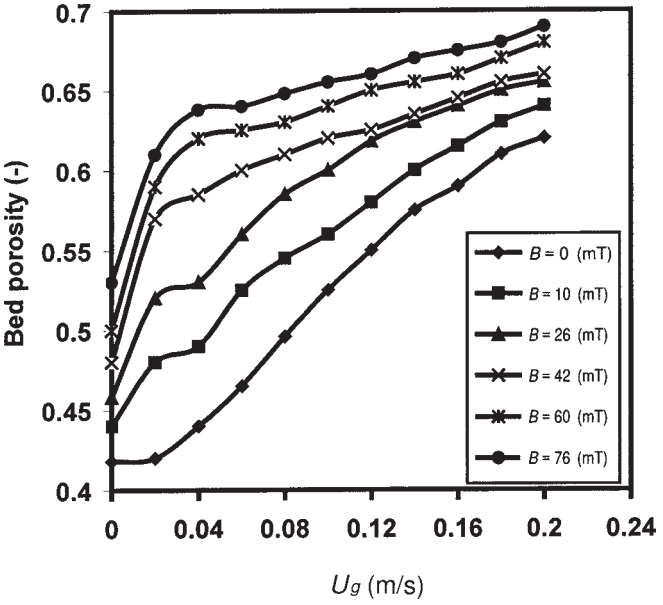

Fig. 4. Effect of magnetic field and fluid velocity on bed porosity for gas-liquid-solid airlift reactor.

Bed Expansion

Bed expansion (bed porosity) is an important property of a fluidized system. It affects the size of the fluid-bed equipment and residence time(s) of the fluid phase(s). In the present case, both the column walls and the supported grid confined the bed. As a result, only axial expansion was possible. The magnetic field also causes anisotropy by arranging the strings along its lines. These physical constraints, in addition to the particle arrangement imposed on the bed structure, are the conditions that determine the changes in the bed structure in the process of slow expansion.

Figure 4 shows bed expansion as a function of gas velocity. An initial expansion occurred in the packed-bed regime directly after the application of the magnetic field and before starting the gas flow. This initial expansion increased as the magnetic field increased. Beyond U_e, the bed started regular expansion as a result of changing its internal structure in response to the simultaneous action of the magnetic cohesive forces between the particles and the gradual increase in the fluid momentum. This process of regular expansion continued until U_{mf} was reached. The bed porosity at the onset of fluidization is the maximum porosity, i.e., ε_{max} that the bed can attain in the stable regime. Beyond U_{mf}, the bed expansion behavior showed no significant differences between that of conventional fluidized beds.

It is evident in Fig. 4 that the rate of increase in bed porosity at low gas velocities was relatively higher than that at high gas velocities. This behavior could be attributed to the fact that the magnetic field tends to distribute uniformly the solids of the bed to cover a height of column equivalent to the

height of the magnetic system. This action starts before starting the fluid flow, as Fig. 4 indicates. As the fluid velocity starts, the magnetic field increases the bed height to approach the height of the magnetic system itself. Most of this expansion occurs at relatively low gas velocities, i.e., $U_g < 0.07$ m/s. Beyond this point, the rate of bed expansion decreases as the bed height approaches the height of the magnetic system. Note that the bed height cannot exceed the height of the magnetic system except at very high gas velocities and low magnetic field intensities, i.e., $U_g > 0.20$ m/s and $B < 35$ mT.

The bed porosity data are correlated in terms of the gas superficial velocity and the magnetic field intensity since the other parameters remain constant. The computer program for curve fitting, Origin, obtains the following empirical relation:

$$\varepsilon = 0.4527 U_g^{0.423} \exp^{0.0077B} \quad (2)$$

In this correlation the range of variables covers U_g from 0.027 to 0.20 m/s and B from 5 to 76 mT because at these conditions an expanded stabilized bed exists. At gas superficial velocities lower than 0.027 m/s, the bed is packed with very low circulation velocity. In addition, if $B < 5$ mT, the resulting magnetic cohesion forces among the particles are weak and do not influence the bed hydrodynamics. The SEE is 0.071.

When the fluid velocity was gradually reduced while maintaining a constant magnetic field intensity, the bed expansion showed hysteresis; that was, the fluidized bed contracted but its porosity remained higher than that at the same conditions when the velocity increases. Even when the fluid throughputs were shut off, the new reformed packed bed remained in a more expanded state than it is at the beginning of the experiment because the magnetic field lines have the ability to hold the magnetic strings in an expanded state. This behavior represent an additional advantage of magnetic stabilization because it is possible to obtain an expanded bed characterized by an improved solid-fluid contact while operating with relatively low gas and liquid flow rates.

Figure 5 shows this hysteresis, which is observed in the bed expansion behavior. It can be seen that the remaining expansion was about 25%, and 50% of the initial bed porosity ($\varepsilon_o = 0.43$) for magnetic field intensities of 42 and 76 mT. This arrangement of the strings is destroyed and the bed returns to its original packed state when the magnetic field is shut off.

Liquid Circulation Velocity

Liquid circulation velocity is a fundamental parameter characterizing three-phase airlift reactors, which is quantified in this study by the downcomer superficial liquid velocity, U_{lc}. This parameter is a function of the operation variables such as gas flow rates, solid size and density, holdup of each phase, and magnetic field intensity.

In the present study, the following criterion, derived when neglecting friction, describes the conditions for which liquid circulation takes place:

$$\varepsilon_g > \varepsilon_s[(\rho_s H_{bo}/\rho_l H_r) - 1] \quad (3)$$

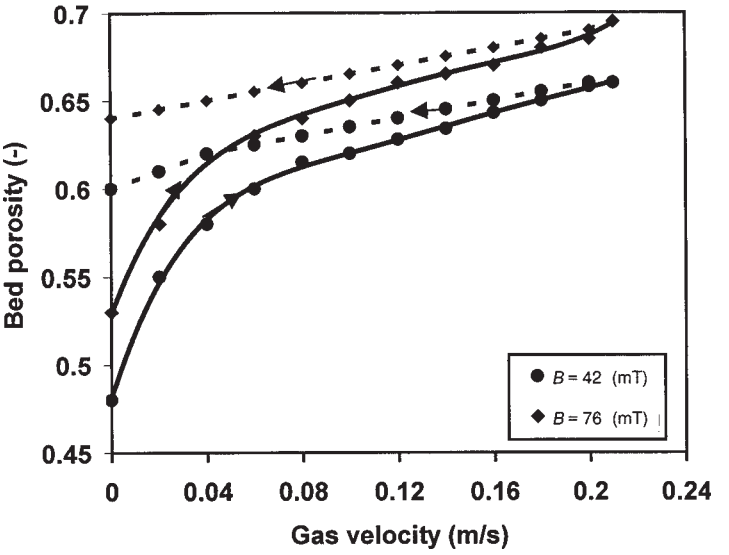

Fig. 5. Bed expansion hysteresis. (——), Increasing flow; (– – –), decreasing flow.

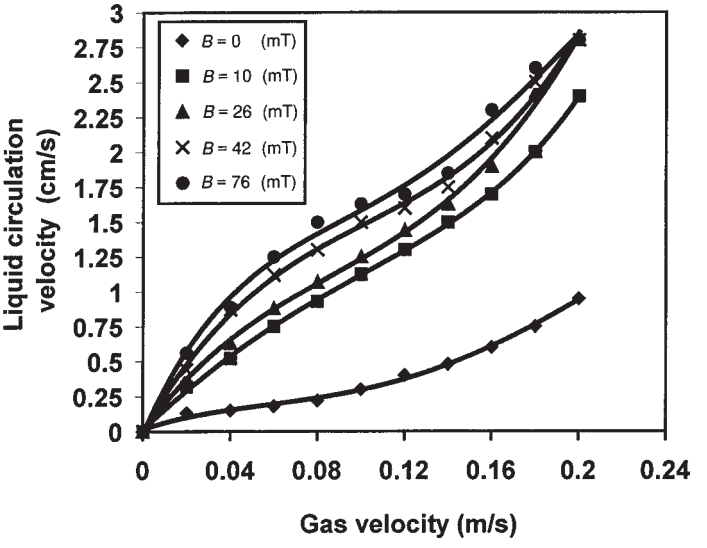

Fig. 6. Effect of magnetic field and gas velocity on liquid circulation velocity.

If the ε_g value is lower than the value implied in this equation, this is an indication that the gas holdup, and hence the pressure drop, between the riser and downcomer is insufficient to induce circulation of liquid and the reactor is said to be "stalled." In a stalled reactor, the solid phase forms a packed bed at the base of the reactor and beneficial contact among the three phases ceases *(31)*.

Figure 6 shows the relation between the gas velocity and liquid circulation velocity, for several magnetic field intensities. The liquid circulation

velocity increased by increasing gas velocity up to the U_e. Beyond this gas velocity, the liquid circulating velocity continued to increase but at a slower rate. This phenomenon is attributed to the agglomeration of the magnetic particles to form chains perpendicular to the fluid flow. More frictional losses among these chains and the circulating liquid will occur in this case. Beyond the minimum fluidization velocity, destruction of the agglomerated chains occurs, and the rate of liquid circulation increases again, in the same manner as in traditional airlift reactors.

It can be seen that in the particulate and strings fluidized regime, liquid circulation velocity values are high and nearly equal to 0.028 m/s. Thus, it can be concluded that in such conditions, liquid circulating velocity depends only on the gas velocity.

Continuous Penicillin Production

Prior to the continuous penicillin production runs, a preliminary set of experiments was performed to determine the maximum possible spore loading on the magnetic beads. The results indicated that the biomass yield was 29, 22, and 20 mg of protein/g of AC1, AC2 and Z beads, respectively. This means that the AC1 provides higher cell concentration than the other two types of bead. In addition, these beads have a relatively low density and are easily fluidized and suspended in the reactor. For these reasons, AC1, i.e., activated carbon magnetic beads (d_p = 0.9 mm) were used to immobilize *P. chrysogenum* for continuous production of penicillin.

Five continuous runs were conducted in the magneto airlift reactor. These runs were conducted under the same conditions. Only the value of the applied magnetic field intensity was varied from run to run. The initial bed height was 0.1 m. In each run, the magnetic field of certain value was applied, and then the flow rate of air was gradually increased until the bed was fluidized. The airflow rate was reduced to a 2.1 cm/s. During this process of increasing the gas velocity to the U_{mf}, and reducing it to a value of 2.1 cm/s, the bed remained in an expanded state under the effect of the magnetic field. Figure 7 shows that the degree of the remaining expansion increased as the magnetic field intensity increased. As a consequence, the residence time of the fresh medium fed to the reactor increased as the magnetic field intensity increased. Each run continued for 120 h. Penicillin production began to decrease after 100–110 h from startup. The reason for this behavior may be because *P. chrysogenum* is a genetically unstable strain and penicillin productivity decreases after a time equivalent from six to seven residence times *(32)*.

Figure 7 shows the variations of the penicillin concentration in the reactor effluent as a function of time at five magnetic field intensities: 0, 10, 17, 23, and 35 mT. It is evident that penicillin concentration increased as the time increased in the first 100 h, then became constant for a short time before it began to decrease. This behavior could be attributed to the fact that the precursor PAA in the medium was being depleted in the first 100 h as indicated by the HPLC analysis. These results agree with those of Jones et al.

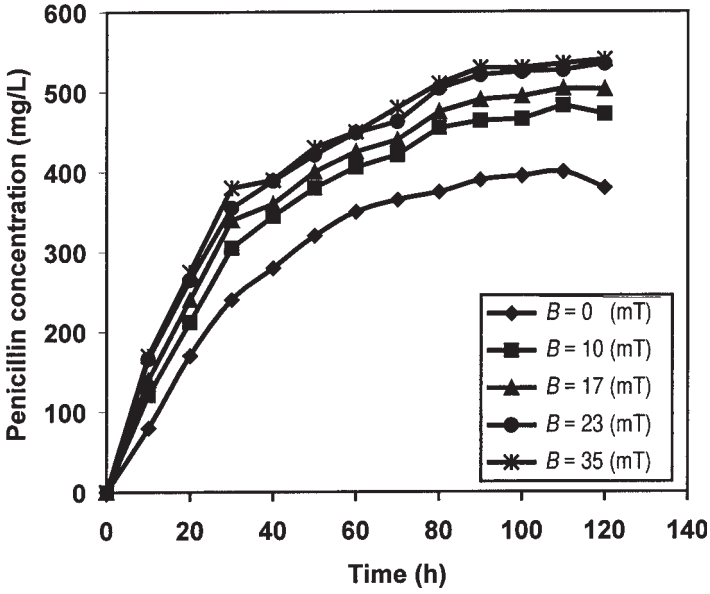

Fig. 7. Variation in concentration of penicillin for different values of magnetic field intensity.

(27). In addition, the applied magnetic field seemed to have a positive effect on penicillin concentration. The maximum penicillin concentration increased from 225 to 333 mg of penicillin/L (48% increase) as the magnetic field intensity increased from 0 to 35 mT. The reason for this effect can be referred to the effect of the magnetic field intensity on the bed height and the bubble sizes in the riser. As shown in Fig. 4, the height of the stabilized bed increases as the magnetic field increases. This means that the substrate residence time in the bed increases as the magnetic field intensity increases. Consequently, the penicillin production rate will increase as the magnetic field intensity increases. In addition, the overall volumetric mass coefficient, $K_L a$ is positively affected by the application of the magnetic field owing to its effect on the gas holdup, bubble sizes, and bed height *(33)*. It is well known that stabilizing the magnetic beads by the field lines reduces the size of the bubble. As a result, the specific surface area, a, of the bubbles increases and their rising velocity decreases as the magnetic field intensity increases.

Figure 8 gives the variation of lactose concentration with time for different magnetic field intensities. Lactose concentration at a time of 100 h decreased from 6.8 to 5.7 g as the magnetic field intensity increased from 0 to 23 mT. This means that substrate utilization in the bed increased as the magnetic field intensity increased. Figure 9 shows how the protein concentration on the magnetic beads varies with time for different magnetic field intensities. It is evident that protein concentration after 100 h of continuous operation increased from 4.0 to 5.45 g as the magnetic field intensity increased from 0 to 35 mT. This is owing to the increase in the effective

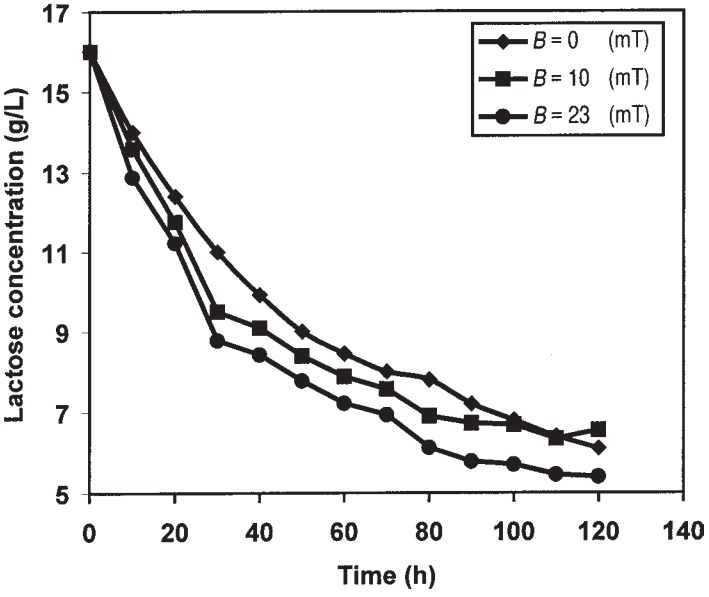

Fig. 8. Effect of magnetic field on lactose concentration in magneto airlift fermentor.

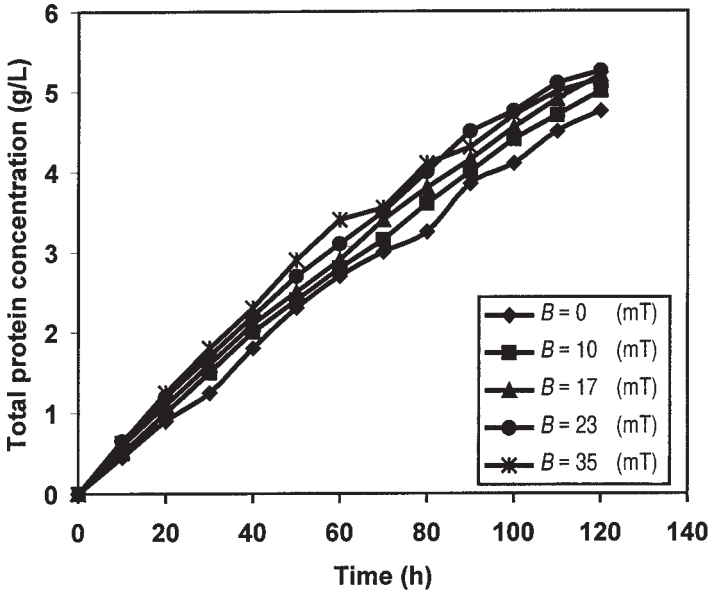

Fig. 9. Effect of magnetic field intensity on total protein concentration in the magneto airlift fermentor.

surface area of the support particles as the bed expands. In addition, aeration of the cells immobilized on the bed particles was improved as the bed expands. Biomass analysis in the effluent medium indicates that there was a limited concentration of free cells in the reactor liquid phase. The total

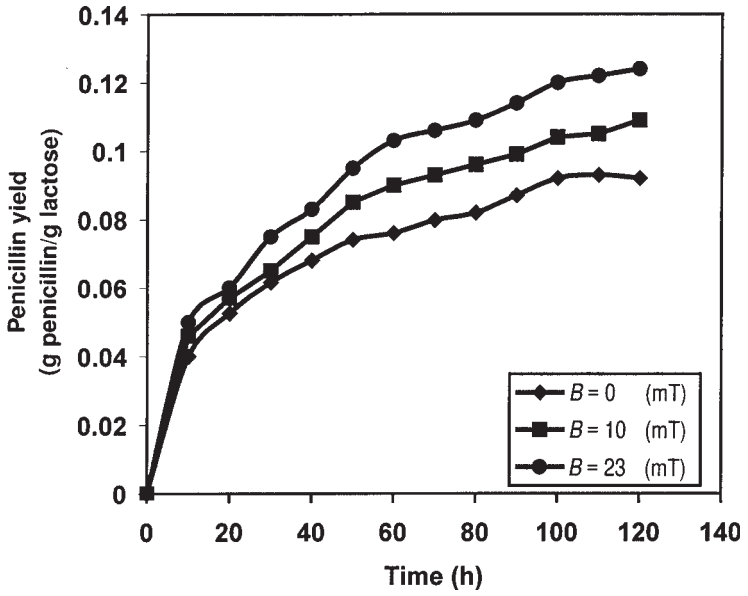

Fig. 10. Penicillin yields in the magneto airlift fermentor for various magnetic field intensities.

amount of free cells in the reactor liquid was at steady state; that is, at 100 h from the start it was about 0.3 g or 5% of the total biomass loaded on the magnetic beads. This indicates that the immobilized cells were strongly attached to the bead surface, and that detachment of these cells occurred at a relatively small rate. This behavior fulfills one of the main assumptions formulated on modeling of continuous processes with immobilized cells; that is, bioconversion by the free cells is negligible compared with that by the immobilized cells. Figure 10 shows that the maximum yield coefficient, $Y_{p/l}$ increased from 0.093 to 0.124 (g of penicillin produced/g of lactose consumed) as the magnetic field intensity increased from 0 to 23 mT.

Note that the role of the magnetic field in the present study was to expand the bed in order to increase the void fraction among the stabilized particles. This helps to increase the biomass concentration on the beads. No adverse effects of the magnetic field on the physiological properties of the microorganism were observed.

Conclusion

Our experiments have allowed an assessment of the effect of a uniform transverse steady magnetic field on the bioproduction of antibiotics by immobilized *P. chrysogenum* on magnetic beads in a three-phase airlift fermenter utilizing a transverse magnetic field. The results show that antibiotic production was improved by the application of the magnetic field owing to the significant changes in the hydrodynamic behavior of magne-

tized beds over conventional systems. These changes can be summarized as follows:

1. The changes in the bed behavior in magnetization first mode can be differentiated into initial packed-bed, stable expanded-bed, and fluidized-bed regimes. The stable expanded bed seems to be an attractive regime for performing bioprocesses with immobilized cells.
2. Bed expansion in the stable regime was regular. The lean zone at the bed surface was eliminated as the magnetic field intensity increased. The maximum bed stable porosity and the remaining expansion increased as the magnetic field intensity increased.
3. The minimum fluidization velocity demarcating the stable and fluidized regimes was found to be strongly dependent on the magnetic field intensity. It could be increased up to seven times as the magnetic field intensity increased from 0 to 76 mT.
4. For a given magnetic field intensity, the liquid circulation velocity increased as the gas velocity increased. The rate of this increase was faster in the fluidized regime than in the stabilized-bed regime.
5. The application of a magnetic field to a three-phase airlift fermentor improved its performance with respect to the yield and conversion.
6. Bioproduction of antibiotics and substrate utilization increased as the magnetic field increased. This can be explained depending on the hydrodynamics of the magneto airlift system.

Nomenclature

A = cross-sectional area of the riser (m^2)
B = magnetic field intensity (mT)
C_p = specific heat (kJ/kg.K)
d_p = particle diameter (m)
H_b = bed height (m)
H_{bo} = initial bed height (m)
H_d = downcomer height (m)
H_r = riser height (m)
K_La = mass-transfer coefficient (m/s)
M_s = saturation magnetic intensity (mT)
U_e = minimum expansion velocity (m/s)
U_g = gas superficial velocity (m/s)
U_{lc} = liquid circulation velocity (m/s)
U_{mf} = minimum fluidization velocity (m/s)
U_{mflo} = minimum fluidization velocity in absence of magnetic field (mT)
U_t = transitional velocity (m/s)
$Y_{p/l}$ = yield coefficient (g of penicillin produced/g of lactose consumed)
ε = bed porosity
ε_g = gas holdup

ε_{max} = maximum porosity
ε_o = initial bed porosity
ε_s = solid holdup
ε_{so} = initial solid holdup
ρ_b = bulk density of magnetic particles (kg/m^3)
ρ_l = liquid density (kg/m^3)
ρ_s = molded density of magnetic particles (kg/m^3)

References

1. Gerda, H. S., Ruud, P. G., Zieleman, G. J., Luyben, K. A., and Kossen, K. A. (1986), *J. Chem. Technol. Biotechnol.* **36,** 335–342.
2. Deckwer, W. D. and Schumpe, A. (1984), *German Chem. Eng.* **7,** 168–177.
3. Prakash, A., Briens, C. L., and Bergougnou, M. A. (1987), *Can. J. Chem. Eng.* **65,** 228–235.
4. Rosensweig, R. E. (1979), *Science* **204,** 57–60.
5. Lee, S. L. P. and Lasa, H. (1988), *Chem. Eng. Sci.* **43(9),** 2445–2449.
6. Penchev, I. P. and Hristov, J. Y. (1990), *Powder Technol.* **61,** 1–11.
7. Filippov, M. V. P. (1960), *Prik Magnet Latvia SSR* **12,** 215–220.
8. Rosensweig, R. E., Siegell, J. H., Lee, W. K., and Mikus, T. (1982), *AIChE Symp. Ser.* **74(205),** 8–16.
9. Siegell, J. H. (1982), *Ind. Eng. Chem. Process Design Dev.* **21,** 135–140.
10. Geuzens, P. and Phoenes, D. (1988), *Chem. Eng. Commun.* **67,** 217–228.
11. Arnaldos, J., Casal, J., and Pugianer, L. (1983), *Powder Technol.* **36,** 33–38.
12. Lee, W. K. (1988), *AIChE Symp. Ser.* **79(222),** 87–96.
13. Sada, E., Katon, S., and Terashima, M. (1981), *Biotechnol. Bioeng.* **23,** 1037–1044.
14. Siegell, J. H., Prickle, J. C., and Dupre, J. D. (1984), *Separation Sci. Technol.* **19,** 977–993.
15. Warrior, M. and Tein, C. (1986), *Chem. Eng. Sci.* **41,** 1711–1721.
16. Rosensweig, R. E., Lee, W. K., and Siegell, J. H. (1987), *Separation Sci. Technol.* **22,** 25–45.
17. Pirckle, J. C., Ruziska, P. A., and Shulk, L. J. (1988), *Chem. Eng. Commun.* **67,** 89–109.
18. Nekrasov, Z. and Chekin, V. (1961), *Izvestia Akad. Nauk. SSR Otdel Tekh Nauk. Met. Toplivo* **6,** 25–32.
19. Penchev, I. P., Al-Qodah, Z., and Hristov, J. Y. (1989), First National Conference on the Application of Fluidized Systems, vol. 1, Plovdiv, Bulgaria, pp. 120–128.
20. Al-Qodah, Z. (1991), PhD thesis, Sofia University of Chemical Technology, Sofia, Bulgaria.
21. Sada, E., Katon, S., Shiozawa, M., and Fukui, T. (1983), *Biotechnol. Bioeng.* **25,** 2285–2292.
22. Hu, T. T. and Wu, J. Y. (1987), *Chem. Eng. Res. Des.* **65,** 238–243.
23. Ivanova, V., Hristov, J., Dobreva, E., Al-Qodah, Z., and Penchev, I. (1996), *Appl. Biochem. Biotechnol.* **59(2),** 187–198.
24. Colin, W., Hong, K., Gillian, M., Richard, W., Angel, M., Jorge, C., Eladia, J., and Mignel, G. (1996), *Chem. Eng. J.* **61,** 241–246.
25. Thompson, V. Z. and Worden, R. M. (1997), *Chem. Eng. Sci.* **52(2),** 279–295.
26. Al-Qodah, Z. (2000), *Can. J. Chem. Eng.* **78(2)**.
27. Jones, A., Wood, D. N., Razniewska, T., and Gaucher, M. (1986), *Can. J. Chem. Eng.* **64,** 547–552.
28. Al-Qodah, Z., Ivanova, V., Dobreva, E., Penchev, I., Hristov, J., and Petrov, R. (1991), *J. Ferment. Bioeng.* **71,** 114–117.
29. Ariyo, B. T., Buke, C., and Kashavarz, T. (1997), *Biotechnol. Bioeng.* **53,** 17–20.
30. Seigel, J. H. (1987), *Powder Technol.* **52,** 139–148.
31. Livingston, A. G. and Zhang, S. F. (1993), *Chem. Eng. Sci.* **48,** 1641–1654.
32. Christensen, L. H., Henriksen, C. M., Nielsen, J., Villadsen, J., and Egelmitani, M. (1995), J. Biotechnol. 42, 95–107.
33. Al-Qodah, Z. and Al-Hassan, M. (2000), *Chem. Eng. J.*, to be published.